Triple-shelled Ni@MnO/C hollow sphere with enhanced performance for rechargeable Zinc-ion capacitor

Tao Xiang,[a] Zaiting Qu,[a] Daohong Zhang,*[a,b] Chenglong Hu,[c] Zhen Chen,[d] Qiufan Wang*[a,b]

[a] Key Laboratory of Catalysis and Energy Materials Chemistry of Ministry of Education & Hubei Key Laboratory of Catalysis and Materials Science, Hubei R&D Center of Hyperbranched Polymers Synthesis and Applications, South-Central Minzu University, Wuhan 430074, China

[b] Guangdong Provincial Laboratory of Chemistry and Fine Chemical Engineering Jieyang Center, Jieyang 515200, China

[c] Key Laboratory of Optoelectronic Chemical Materials and Devices, Ministry of Education, School of Optoelectronic Materials and Technology, Jianghan University, Wuhan 430056, China

[d] College of Chemical and Environmental Engineering, Hanjiang Normal University, Shiyan 442000, China

Email: daohong.zhang@mail.scuec.edu.cn (D. Zhang); ygdf@mail.scuec.edu.cn (Q. Wang)

Characterization:

The phase purity of the synthesized samples was identified by X-ray diffraction (XRD). The morphologies of the products were studied by scanning electron microscopy (SEM) and transmission electron microscopy (TEM).

Electrochemical Measurements:

The Ni/MnO@C cathode for ZIBs was prepared by mixing Ni/MnO@C, Super P, and polyvinylidene fluoride (PVDF) in a weight ratio of 7:2:1 in N-methyl-2-pyrrolidone solvent. The slurry was then coated onto carbon cloth and vacuum-dried at 80°C for 10 hours. CR2032 coin cells were assembled using zinc foil as the anode, non-woven fabric as the separator, and a 2 M $ZnSO_4$ + 0.2 M $MnSO_4$ electrolyte solution.

Electrochemical evaluations were conducted using the same assembly method for comparative samples. Charge-discharge measurements within a voltage window of 1.0 to 1.9 V were performed using a Neware battery testing system (Shenzhen, Neware, China). For comparison, galvanostatic charge-discharge (GCD) tests were also conducted within a 1.0 to 1.8 V voltage window. Cells tested within the 1.0-1.9 V voltage window were labeled as activated Ni/MnO@C, while the control group was labeled as non-activated Ni/MnO@C. For the Galvanostatic Intermittent Titration Technique (GITT) tests, the current pulse was sustained for 20 min at 100 mA g^{-1} and then without current for 30 min. The Zn^{2+} diffusion coefficient (D) is determined based on the following equation:

$$D = \frac{4L^2}{\pi\tau}\left(\frac{\Delta Es}{\Delta E\tau}\right)^2$$

Where τ corresponds to the time of constant current pulse, L is the electrode thickness, ΔEs represents the voltage change caused by the current pulse, and ΔEτ is the cell voltage change that arises from galvanostatic charge/discharge.

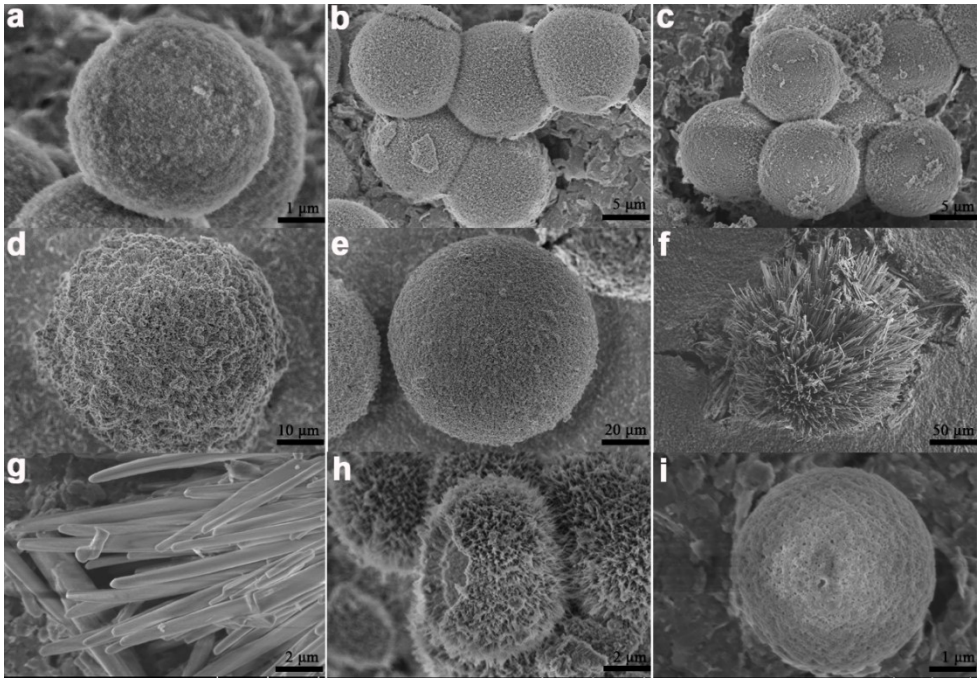

Figure S1. (a) SEM image of Ni-MOFs, (b) SEM image of $Ni_{10}Mn_1$-MOFs, (c) SEM image of Ni_3Mn-MOFs, (d) SEM image of Ni_1Mn_1-MOFs, (e) SEM image of

Ni_1Mn_3-MOFs, (f) SEM image of $NiMn_{10}$-MOFs, (g) SEM image of Mn-MOFs, (h) SEM image when the reaction solvent without ethylene glycol, (i) SEM image when the reaction solvent only contains ethylene glycol.

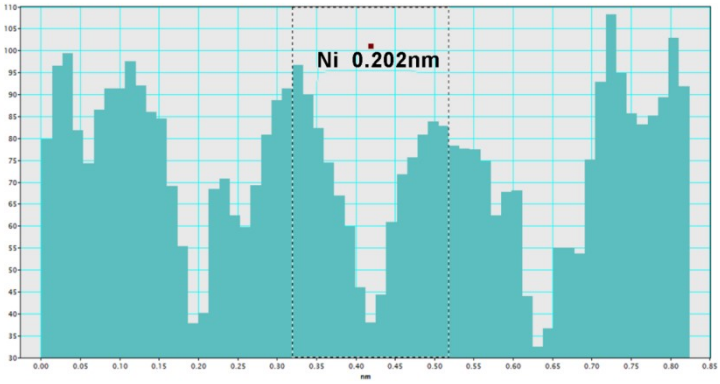

Figure S2. Lattice distance image of Ni.

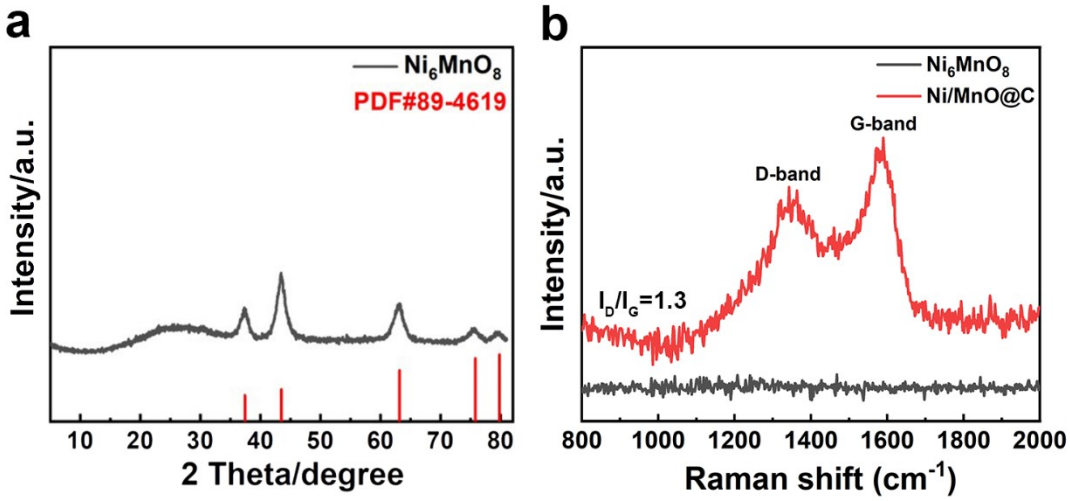

Figure S3.(a) XRD patterns of Ni_3Mn_1-MOFs calcined at 400°C in O_2. (b) Raman spectrum.

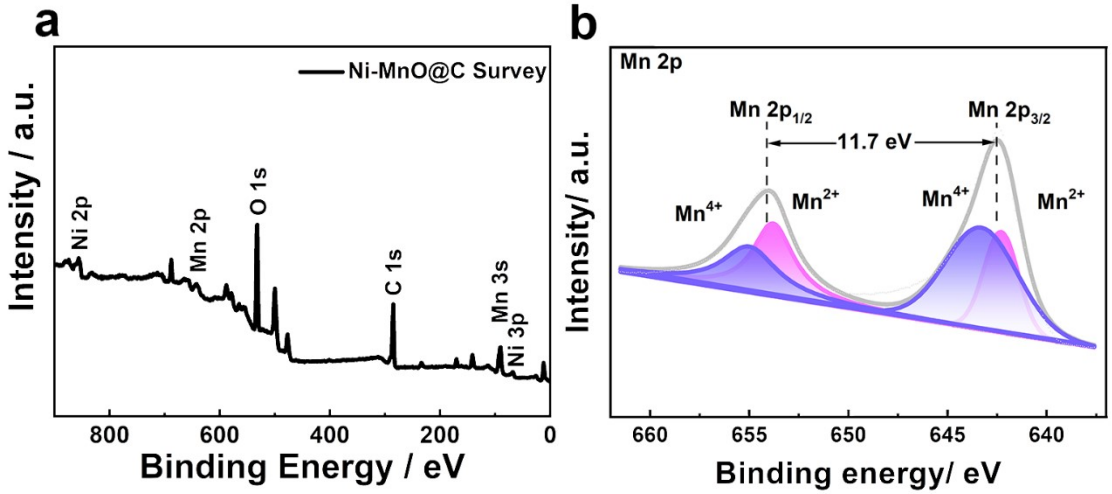

Figure S4. (a) XPS survey spectrum and (b) Mn 2p.

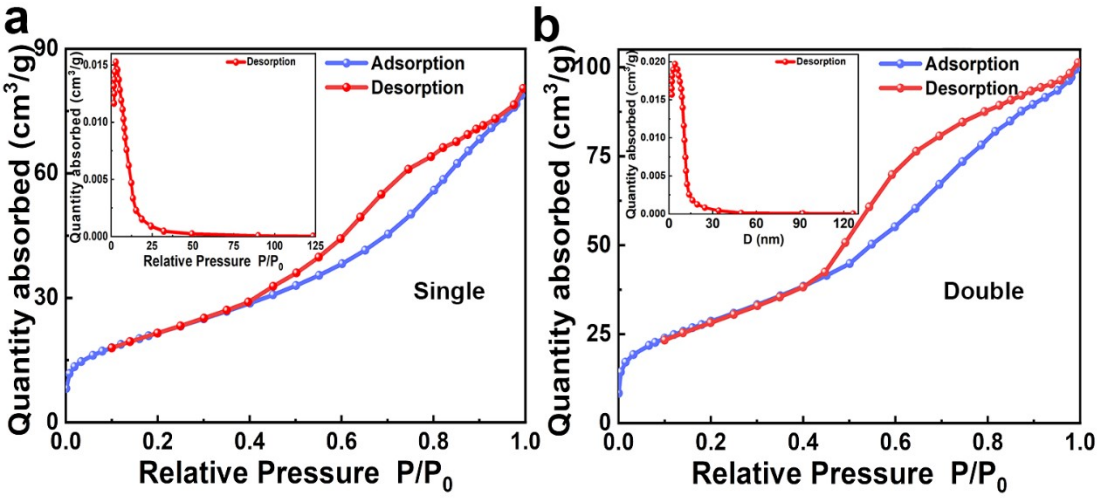

Figure S5. Nitrogen adsorption-desorption curve and pore-size distribution of (a) the single-shelled and (b)double-shelled Ni/MnO@C.

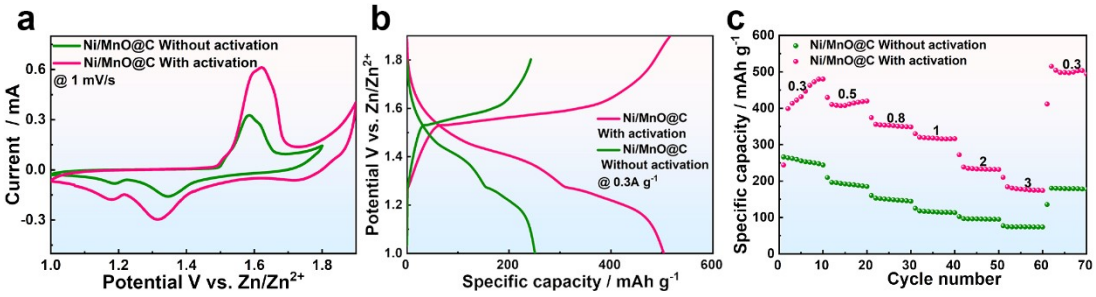

Figure S6. Electrochemical properties of Ni/MnO@C cathodes. a) CV curves of Ni/MnO@C within different voltage range at 1 mV s^{-1}. b) GCD curves of Ni/MnO@C at 0.3 A g^{-1} within different voltage range. c) Rate performance of Ni/MnO@C with/without activation.

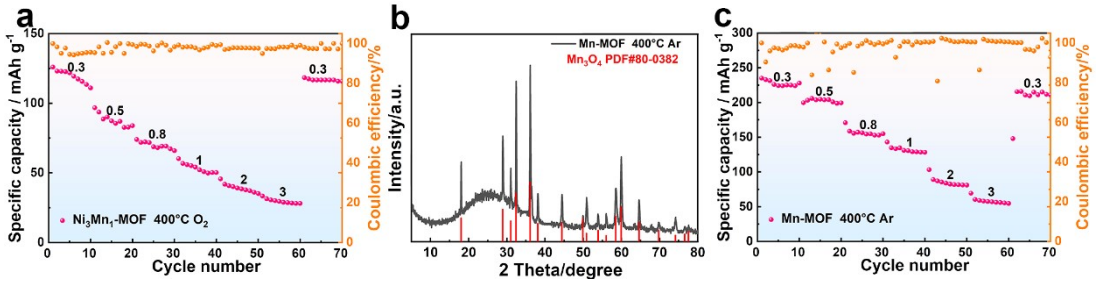

Figure S7. (a) Rate capability of Ni_3Mn_1-MOFs calcined at 400 ° C under O_2 conditions. (b) XRD patterns of Mn-MOFs calcined at 400°C in Ar. (c) Rate capability of Mn-MOFs calcined at 400 ° C in Ar atmosphere.

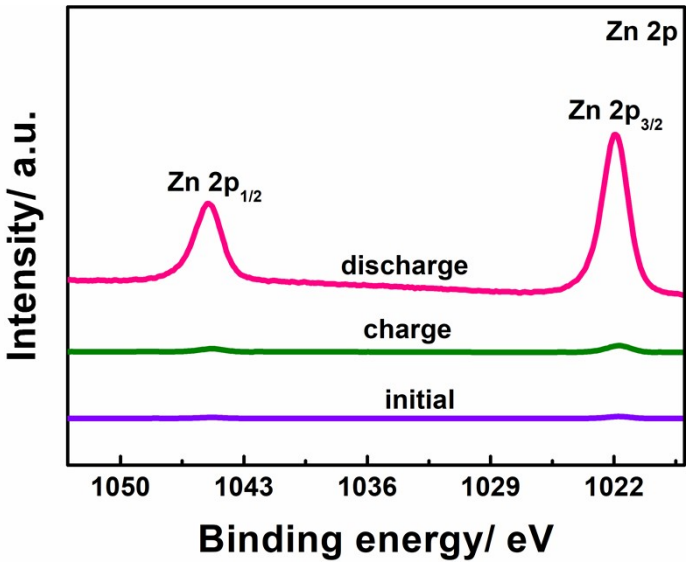

Figure S8. Ex situ XPS spectrum of Zn 2p.

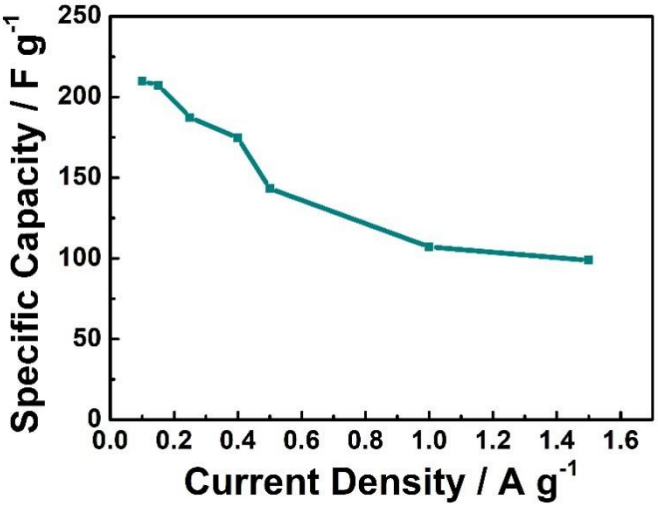

Figure S9. Capacities of the devices at different current densities.